EurJIC
European Journal of Inorganic Chemistry

Research Article
doi.org/10.1002/ejic.202200562

Chemistry Europe
European Chemical Societies Publishing

www.eurjic.org

VIP *Very Important Paper*

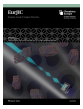

Isostructural Family of Rare-Earth MOFs Synthesized from 1,1,2,2-Tetrakis(4-phosphonophenyl)ethylene

Felix Steinke,[a] Tobias Otto,[a] Sho Ito,[b] Stephan Wöhlbrandt,[a] and Norbert Stock*[a, c]

The tetraphosphonic acid 1,1,2,2-tetrakis(4-phosphonophenyl)ethylene (H_8L) was used as linker in the synthesis of eight new isostructural, phosphonate-based metal-organic frameworks of composition $[M_2(H_2O)_2(H_2L)]\cdot xH_2O$ ($M{=}Y^{3+}$, Tb^{3+}, Dy^{3+}, Ho^{3+}, Er^{3+}, Tm^{3+}, Yb^{3+}, Lu^{3+}; $1.5 < x < 4$), denoted as **M-CAU-34**. The compounds were synthesized under hydrothermal reaction conditions, using the corresponding metal nitrates as starting materials. The determination of the crystal structure was achieved by a combination of electron and powder X-ray diffraction (PXRD) data. In addition, a thorough characterization by thermogravimetric and elemental analysis, IR- and Raman-spectroscopy as well as H_2O-sorption is given.

Introduction

Metal-organic frameworks (MOFs) exhibit modular compositions, in which inorganic and organic building units can be selected to influence the properties of the resulting materials. Especially the high variability in the choice of linker molecules can have a significant impact on the resulting framework structure and properties.[1] While the field of MOF research is steadily growing and expanding into various fields of applications, such as sensing,[2] molecular separation[3] or catalysis,[4] carboxylate based compounds overwhelmingly make up the majority of studied MOFs. The use of linker molecules containing other functional groups such as phosphonic acids have attracted less attention.[5] This is due to a preferred formation of dense and layered structures[6] and the necessity of linker synthesis since only a limited number of suitable phosphonic acids are commercially available.

Different studies have demonstrated the use of di-, tri- and tetraphosphonic acids for the synthesis of phosphonate based MOFs.[7] While the use of diphosphonic acids often rely on serendipity and exploratory investigations, the use of large tri- or tetratopic linker molecules resulted in porosity through the arrangement of space demanding linker molecules.[8] As part of these studies, our group recently reported the successful use of 1,1,2,2-tetrakis(4-phosphonophenyl)ethylene (H_8L, Figure 1) as a starting material for the synthesis of porous metal phosphonates in combination with divalent metal ions.[9] The suitability of this linker for the synthesis of new MOFs was confirmed in studies using trivalent metal ions, which included group 13 and transition metal ions.[10]

Phosphonate based MOFs have also a tendency to crystallize as microcrystalline powders.[11,12] Recent advances in electron diffraction in combination with PXRD proofed this method as an excellent tool to achieve structure determination of these types of microcrystalline samples.[11–13] One of the main complications of electron diffraction in MOF investigation is beam damage,[14] which can render the determination of correct structural models extremely difficult by negatively impacting the data quality. However, commercial applications of electron diffraction are getting more common. The XtaLAB Synergy-ED by Rigaku and JEOL is the first commercially available dedicated electron diffractometer, which allows users solving crystal structures of nano-sized crystallites from electron diffraction much more easily, making the method more readily accessible to the crystallographic community.

Herein we report the use of yttrium and seven lanthanoid salts in the synthesis of new isostructural, microcrystalline

[a] *F. Steinke, T. Otto, Dr. S. Wöhlbrandt, Prof. Dr. N. Stock*
Institute of Inorganic Chemistry
Christian-Albrechts-Universität zu Kiel
Max-Eyth-Str. 2, 24118 Kiel, Germany
E-mail: stock@ac.uni-kiel.de
https://www.ac.uni-kiel.de/de/stock
[b] *S. Ito*
Rigaku Corporation
3-9-12 Matsubara-cho, Akishima, Tokyo 196-8666, Japan
[c] *Prof. Dr. N. Stock*
Kiel Nano, Surface and Interface Science KiNSIS,
Christian-Albrechts-Universität zu Kiel
Christian-Albrechts-Platz 4, 24118 Kiel, Germany

Supporting information for this article is available on the WWW under https://doi.org/10.1002/ejic.202200562

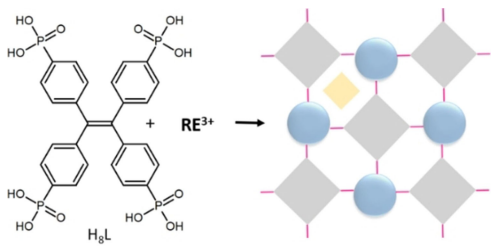

Figure 1. The reaction of the linker molecule 1,1,2,2-tetrakis(4-phosphonophenyl)ethylene (H_8L, left) with several rare-earth (RE) nitrates leads to the formation of metal phosphonates of composition $[M_2(H_2O)_2(H_2L)]\cdot xH_2O$ ($M{=}Y^{3+}$, Tb^{3+}, Dy^{3+}, Ho^{3+}, Er^{3+}, Tm^{3+}, Yb^{3+}, Lu^{3+}), denoted **CAU-34**, under hydrothermal synthesis conditions. Color scheme: grey = linker, blue = IBU, yellow = pore.

Research Article
doi.org/10.1002/ejic.202200562

phosphonate based MOFs denoted as M–**CAU-34** (M=Y^{3+}, Tb^{3+}, Dy^{3+}, Ho^{3+}, Er^{3+}, Tm^{3+}, Yb^{3+}, Lu^{3+}) (Figure 1).

Results and Discussion

Synthesis of M-CAU-34

The synthesis of **Y-CAU-34** was easily accomplished under hydrothermal reaction conditions at 150 °C within 12 hours, using yttrium nitrate and the linker molecule in water as the solvent in a molar ratio $M^{3+}:H_8L:H_2O = 2:1:3700$. The compound was first synthesized at a 1 mL scale, while the scale-up to the 10 mL scale was also achieved. **Y-CAU-34** was obtained as a microcrystalline product and therefore structure determination was carried out by a combination of electron diffraction (ED) and powder X-ray diffraction (PXRD).

A metal screening experiment was carried out using our in-house high-throughput setup, in order to study the effect of the ionic radius on the product formation. Hence yttrium nitrate was replaced by 14 lanthanoid nitrates while all other synthesis parameters were kept the same. The PXRD patterns of the reaction products are shown in Figure 2. **CAU-34** is also formed with the seven other rare-earth ions Tb, Dy, Ho, Er, Tm, Yb and Lu, although the samples containing Tb and Lu contain minor impurities as proven by LeBail fits of the PXRD data (Figures S11 and S12). As a general trend, significant peak broadening is observed with increasing atomic number, i.e. decreasing ionic radius. The use of the other rare-earth ions (Ce to Gd) under these reaction conditions results in the formation of products of low crystallinity or a highly crystalline compound when La is used. This compound crystallizes in a different structure and it is therefore not discussed in the manuscript. Only phase pure **CAU-34** compounds were further characterized in detail.

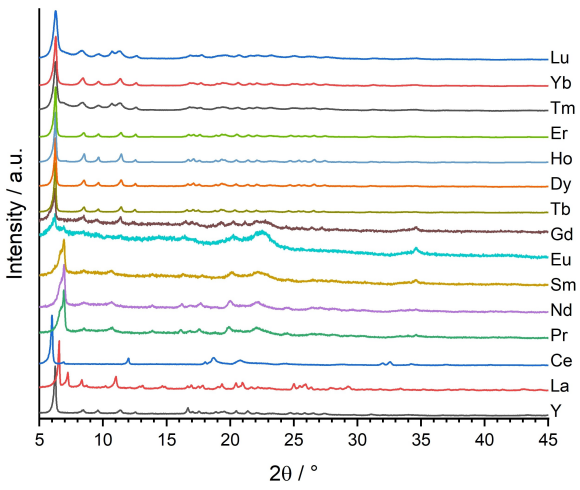

Figure 2. PXRD data of reaction products obtained in a high-throughput screening experiment using 15 different rare-earth nitrates.

Crystal structure determination of Y-CAU-34

Although several attempts were made to solve the crystal structure of **Y-CAU-34** *ab initio* from PXRD data, no structure model suitable for a structure refinement employing the Rietveld method could be obtained. Therefore, electron diffraction was employed to solve the crystal structure. The obtained structural model was refined using the Rietveld-algorithm as implemented in Topas Academics.[15] Distance restrains were used to refine the position of yttrium, oxygen and phosphorous atoms. The carbon backbone of the linker molecule was refined employing a z-matrix with constraints for bond lengths and angles. Adsorbed water molecules in the pores were considered and refined as oxygen atoms on general positions. PXRD data of the lanthanide analogues of **Y-CAU-34** were refined using the Le Bail algorithm to confirm phase purity and to refine the lattice parameters The final crystallographic data of the refinements of **M-CAU-34** (**M=Y**, **Tb**, **Dy**, **Ho**, **Er**, **Tm**, **Yb**, **Lu**) are given in Tables S1–S2 and the respective plots are shown in S5–S12.

Crystal structure description of Y-CAU-34

The asymmetric unit of $[Y_2(H_2O)_2(H_2L)]\cdot 4H_2O$ consists of half a linker molecule on a special position, one Y^{3+} ion on a general position as well as one coordinating water molecule (Figure 3a). Additionally, there are two water molecules located in the pores. Each metal ion is surrounded by six oxygen atoms originating from five different linker molecules and a seventh oxygen atom, assigned to a coordinating water molecule, which leads to a pentagonal bipyramidal coordination environment. Each linker is connecting ten Y^{3+} ions. The interconnection of the phosphonate groups can be described using the Harris notation as [2.110] and $[3.2_{12}1_21_3]$ for the phosphorus atoms P11 and P21, respectively (Figure 3c).[16] According to the Harris notation, there are two non-coordinating phosphonate oxygen atoms in each linker molecule, which are likely protonated. Localization of the proton, which is necessary for charge balance, was not possible, since the structure refinement was carried out against PXRD data. The Y–O and P–O bond lengths of the IBU (Figure 3b) and C–P bond lengths are given in Table S3. The values are within the range observed for other yttrium phosphonates reported in the CSD MOF subset as analyzed using Conquest and Mercury.[17] The inorganic building unit (IBU) is formed by edge sharing YO_7-polyhedra (Figure 3c), which are interconnected though phosphonate groups to rods along the *b*-axis. This type of IBU with periodicity along one direction was previously reported for metal(III) phosphonates.[18] Each rod is connected through four linker moieties to eight other rods along the *a*- and the *c*-axis forming a (I^1O^2)-3D-network, according to the classification scheme (I^nO^m) proposed by Cheetham, which describes the dimensionality of different structures with respect to both organic connectivity between metal centers (O^m) and extended inorganic connectivity (I^n).[19]

The general structural motif with each linker interconnecting four IBUs is also found in cobalt and aluminum phospho-

Research Article
doi.org/10.1002/ejic.202200562

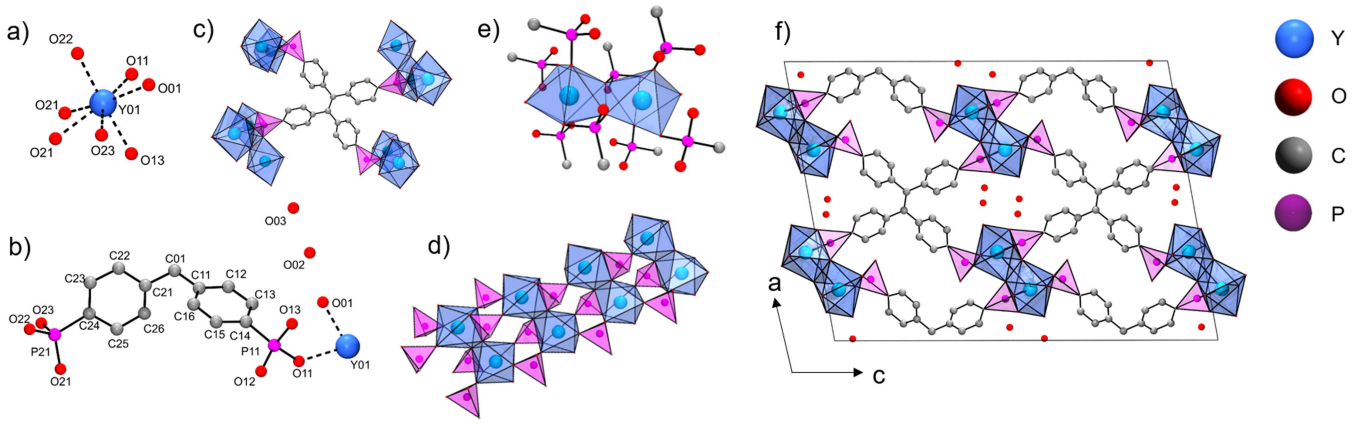

Figure 3. Crystal structure of **Y-CAU-34**. a) Pentagonal bipyramidal coordination environment of Y^{3+} ions, b) asymmetric unit, c) connection of Y^{3+} ions by a linker molecule, d) representation of the rod-shaped inorganic building unit (IBU), e) edge-sharing dimers in the IBU of **CAU-34** and coordinated phosphonate groups interconnecting the dimers, f) representation of the crystal structure as seen along the *b*-axis.

nates CAU-48[9] and CAU-53.[10] The motif was predicted for metal phosphonates composed of a square-shaped geometry and chain-type IBUs.[12] In the crystal structure of **CAU-34**, channel-type ultra-micro pores are found with a limiting pore diameter of 2.48 Å, while the maximum diameter is 3.5 Å as determined with the program PoreBlazer.[22]

Since the limiting diameter is below, but in the range of the kinetic diameter of water molecules, uptake of water at 298 K is anticipated but the adsorption of the bigger nitrogen molecules at 77 K is not expected.[23] In the as synthesized **CAU-34**, the channels are filled with physisorbed water molecules.

The lattice parameters of the other isostructural compounds **Ln-CAU-34** (**Ln**=**Tb**, **Dy**, **Ho**, **Er**, **Tm**, **Yb**, **Lu**) were determined by Le Bail refinements and are listed in Tables S1 and S2. A plot of the ionic radius against the volume of the unit cell is shown in Figure 4 and an increase with the ionic radius is found. Since **Tb-** and **Lu-CAU-34** are not phase-pure according to the PXRD data, these compounds were not further characterized.

Thermal properties

The purity of the synthesized compounds **Y-CAU-34** and **Ln-CAU-34** (**Ln**=**Dy**, **Ho**, **Er**, **Tm**, **Yb**) was further confirmed by elemental analysis (see experimental) and thermal properties were determined by thermogravimetric (TG) measurements (Table 1, Figure 5, Figures S13–S18). The TG curves show the expected loss of water molecules between 100 and 290 °C in one or two weight loss steps, which are not well resolved, followed by the exothermic decomposition of the linker molecule at temperatures ranging from 380–440 °C in several steps. The calculated mass losses of adsorbed and coordinating water molecules are in accordance with the results from the elemental analysis (Table 1). After the TG measurements, the residues were analyzed by PXRD. They are composed of different mixtures of metal phosphates ($M(III)PO_4$, $M(III)(PO_3)_3$) and also contain unidentified phases.

The thermal stability of the crystal structure of **Y-CAU-34** was studied employing variable temperature (VT-) PXRD measurements (Figure S19). Only minor structural changes are

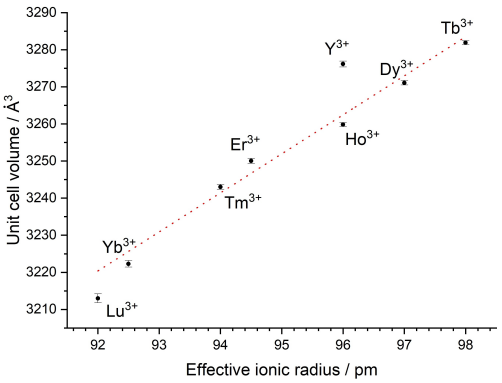

Figure 4. Evolution of the unit cell volume of the title compounds depending of the crystal ionic radii of the used rare-earth ion with coordination number seven.[20,21] The unit cell volumes were obtained from Rietveld and Le Bail refinements using PXRD data.

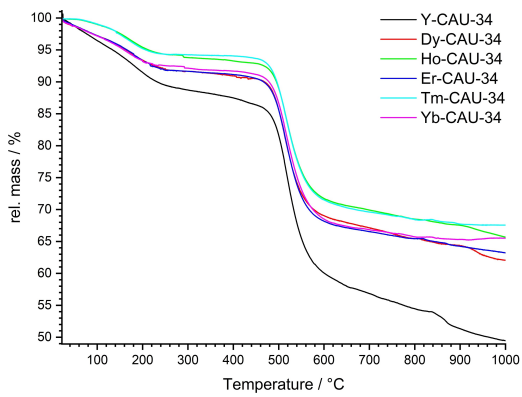

Figure 5. TG-data of **M-CAU-34** in the range of 30 to 1000 °C (M=Y^{3+}, Dy^{3+}, Ho^{3+}, Er^{3+}, Tm^{3+}, Yb^{3+}).

Research Article
doi.org/10.1002/ejic.202200562

Table 1. Results of the elemental and TG analysis as well as H_2O-sorption measurement of **M-CAU-34** ($[M_2(H_2O)_2(LH_2)]\cdot xH_2O$; M=Y, Dy, Ho, Er, Tm, Yb). The mass loss of adsorbed and coordinating water molecules as well as the temperature range for the loss of water and the decomposition temperature of the linker is given. For the H_2O adsorption, the water uptake in mol/mol and mg(H_2O)/g(CAU-34) is given.

	Elemental analysis			TG analysis		H_2O uptake in adsorption measurement	
Sum formula	observed/ calculated	Mass loss H_2O [%] (obs./calc.)	H_2O molecules per sum formula	Temperature range for the loss of water [°C]	Onset temperature for the decomposition of the linker [°C]	mg(H_2O)/ g(CAU-34)	mol/mol
$[Y_2(H_2O)_2(LH_2)]\cdot 4H_2O$	C 34.6/33.5, H 3.36/3.24	11.9/11.6	6	20–280	400	120	6.3
$[Dy_2(H_2O)_2(LH_2)]\cdot 3.5H_2O$	C 30.0/29.7, H 2.91/2.59	7.71/7.70	5.5	20–265	440	83	5.1
$[Ho_2(H_2O)_2(LH_2)]\cdot 2H_2O$	C 30.1/29.8, H 2.84/2.42	6.51/6.07	4	20–290	430	64	3.9
$[Er_2(H_2O)_2(LH_2)]\cdot 3H_2O$	C 29.5/29.2, H 2.94/2.64	8.62/8.41	5	20–260	390	89	5.6
$[Tm_2(H_2O)_2(LH_2)]\cdot 1.5H_2O$	C 29.4/29.8, H 2.95/2.41	5.85/6.02	3.5	20–250	380	68	4.2
$[Yb_2(H_2O)_2(LH_2)]\cdot 3H_2O$	C 29.3/28.9, H 2.92/2.61	8.07/8.32	5	20–250	400	124	7.8

observed between 30 and 350 °C, followed by the loss of long-range order and decomposition.

Sorption measurements

The sorption behavior of the **Y-CAU-34** was investigated using nitrogen, carbon dioxide and water as the adsorptive (Figure 6). H_2O and CO_2 sorption isotherms were recorded at 298 K, while N_2 isotherms were collected at 77 K.

For the isostructural compounds, only H_2O sorption isotherms were recorded (Figure S22). Prior to the measurements the samples were thermally activated at 120 °C under reduced pressure over night. PXRD patterns were collected after each measurement to confirm the preservation of long-range order (Figure S25 to S30). All compounds show an uptake of water during the adsorption measurements. **Y-CAU-34** shows a steep uptake of water at low relative humidity ($0 < p/p_0 < 0.037$). This first uptake of three water molecules per formula unit (ca. 5.7 wt-%) is followed by the uptake of three water molecules per formula up to $p/p_0 = 0.80$. The total uptake of 6.3 water molecules is slightly higher than expected from the TGA results, which may be attributed to the high relative humidity during the measurement. The total water uptake of the isostructural compounds ranges between 3.9-7.8 mol/mol (Table 1).

Y-CAU-34 shows no significant uptake of N_2 at 77 K, however, CO_2 is adsorbed to a small extent at 298 K.

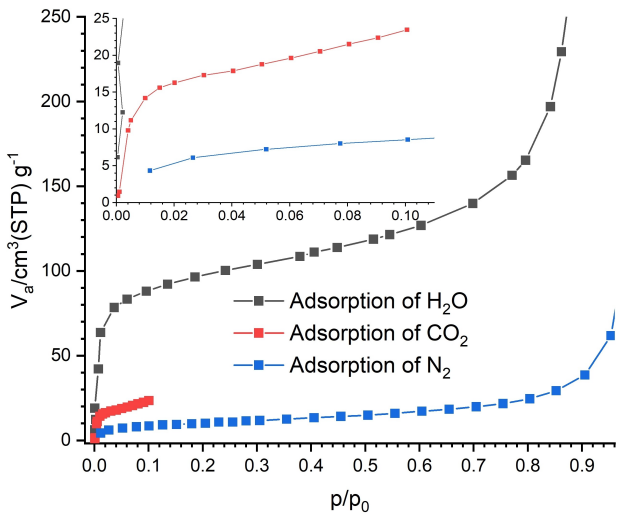

Figure 6. H_2O (black), CO_2 (red) and N_2-(blue) adsorption isotherms of **Y-CAU-34** measured at 298 K (H_2O and CO_2) or 77 K (N_2) after activation at 120 °C in 16 hours under reduced pressure. A specific surface area of $a_{BET} = 37\ m^2/g$ was calculated from the nitrogen adsorption data.

Conclusion

The use of the tetratopic linker molecule 1,1,2,2-tetrakis(4-phosphonophenyl)ethylene and rare-earth metal ions in syntheses deploying hydrothermal reaction conditions led to the discovery of eight new porous metal phosphonates denoted **M-CAU-34** (M=Y, Tb, Dy, Ho, Er, Tm, Yb, Lu). The crystal structure of **Y-CAU-34** was solved from electron diffraction data and successfully refined against PXRD data. Le Bail fits were used to confirm the purity and the lattice parameters of the other isostructural **CAU-34** compounds. As expected, an increase in the unit cell volume with increasing ionic radius is observed. Rare-earth ions with an effective radius larger than 98 pm lead to less crystalline products or a different crystal structure. The title compounds show water adsorption at low p/p_0 values, indicating high hydrophilicity. For **Y-CAU-34**, a high thermal stability of 350 °C was observed by VT-PXRD measurements.

Experimental Section

Materials and methods

A list of starting materials and solvents is given in the SI (Table S5). If not noted otherwise, all chemicals were used as received from

commercial sources without further purification. $NiCl_2 \cdot 6H_2O$ was heated in an oven at 150 °C for 24 hours prior to the linker synthesis to receive anhydrous $NiCl_2$. Powder X-ray diffraction (PXRD) data were collected on a Stoe Stadi P-Combi and on a Stadi MP diffractometer both equipped with a MYTHEN 1 K detector ($CuK_{\alpha 1}$-radiation, $\lambda = 1.5406$ Å) in transmission using an xy- or flat sample holder. IR-spectra were measured on a Bruker ALPHA-FT-IR A220/D-01 using an ATR-unit. Raman spectra were recorded at RT on a Bruker RAM II FT-Raman spectrometer using a liquid nitrogen cooled, highly sensitive Ge detector, 1064 nm radiation and 3 cm^{-1} resolution. ^{1}H- and ^{31}P-NMR spectra were recorded with a Bruker AVANCE III HD Pulse Fourier Transform spectrometer equipped with a cryo-probehead Prodigy BBO400S1 BB-H&F-D-05-Z operating at a frequency of 400.13 MHz (^{1}H) or 161.98 MHz (^{31}P). The CHNS-measurements were performed with a vario MICRO cube Elementaranalysator from Elementar. Thermogravimetric and DSC data was collected on a Linseis STA PT 1600 (airflow = 6 L/h, heating rate = 4 K min^{-1}). Variable temperature PXRD data (VT-PXRD) was collected with a Stoe capillary furnace in a 0.5 mm quartz capillary. The temperature range between 30 °C and 500 °C was studied. The samples were heated in steps of 10 °C (30–400 °C) or 20 °C (400–500 °C). Sorption measurements were carried out using a BEL Japan Inc. BELSORP-max with water vapor at 298 K and a BELSORP-MiniX with N_2 or CO_2 at 77 or 298 K respectively. The samples were treated for 16 h at 120 °C under reduced pressure ($p < 10^{-2}$ mbar) prior to the measurements. The syntheses of the title compounds was carried out in a programmable Memmert UNB 500 oven with forced ventilation using custom-made steel autoclaves with Teflon inserts (total volume of 2 or 20 ml).[24] Electron diffraction data was collected using a Rigaku XtaLAB Synergy-ED diffractometer equipped with a Rigaku HyPix-ED detector and LaB_6 electron source at 200 keV, in vacuum at ambient temperature.[25]

Synthesis

Synthesis and characterization of 1,1,2,2-tetrakis(4-phosphonophenyl)ethylene

The linker molecule 1,1,2,2-tetrakis(4-phosphonophenyl)ethylene was synthesized as described in literature.[9] In a first step, 1,1,2,2-tetrakis(4-bromophenyl)ethylene was synthesized starting from 1,1,2,2-tetraphenylethylene and bromine. In a second step, the brominated product was phosphonated in a nickel-catalyzed reaction using triethylphosphite. The linker was obtained by hydrolysis using concentrated hydrochloric acid as a white powder (6.65 g, 55% yield based on tetrabromophenylethylene). ^{1}H- and ^{31}P-NMR spectra are given in the SI (Figure S1).

^{1}H-NMR (400 MHz, 300 K, NaOD/D_2O (10%)): $\delta = 7.06$ (dd, J = 11.3/8.0 Hz, 8H), 6.73 (dd, J = 8.1 Hz, 8H), ppm.

^{31}P-NMR (162 MHz, 300 K, NaOD/D_2O (10%)): $\delta = 11.1$ ppm.

Synthesis of Y-CAU-34 $[Y_2(H_2O)_2(C_{26}H_{16}P_4O_{12}H_2)] \cdot 3H_2O$

The title compound was first synthesized using our high-throughput setup[24] following the procedures reported in our previous studies with other di- and trivalent metal ions.[9,10] Thus in a 2 mL Teflon insert, 30 µL (0.03 mmol, $c = 1$ mol L^{-1}) of an aqueous solution of yttrium nitrate, 1,1,2,2-tetrakis(4-phosphonophenyl)ethylene (0.015 mmol, 9.8 mg) and 970 µL H_2O were combined. After sealing the multiclave, the reaction was carried out by heating the mixture to 150 °C within one hour and keeping this temperature for 12 hours. After cooling to room temperature, the product was isolated by filtration, rinsed three times with 2 mL of water and methanol, respectively, and finally dried under ambient conditions. **Y-CAU-34** was obtained as white microcrystalline powder.

For the characterization of the new compound, a scale-up of the synthesis was necessary, which was easily achieved. 1,1,2,2-tetrakis(4-phosphonophenyl)ethylene (0.15, mmol, 97.9 mg) was transferred into a 30 mL Teflon insert and 9.7 mL H_2O and an aqueous solution of yttrium nitrate (0.3 mmol, 300 µL, 1 mol L^{-1}) were added. The Teflon insert was enclosed in a steel autoclave and heated to 150 °C within 1 hour, kept at this temperature for 12 hours and cooled down to room temperature. The product was isolated through vacuum filtration, washed with 20 mL H_2O and methanol, respectively, and dried at ambient conditions in air. 124 mg (0.119 mmol, 79.1%) **Y-CAU-34** were obtained.

Results of the elemental analyses (observed/calculated): C 34.6/33.5, H 3.36/3.24 (calculated for $[Y_2(H_2O)_2(C_{26}H_{16}P_4O_{12}H_2)] \cdot 4H_2O$)

Synthesis of Ln-CAU-34 (Ln=Dy, Ho, Er, Tm, Yb, Lu)

The lanthanide analogues of **Y-CAU-34** were obtained by using the respective metal nitrate, following the synthesis procedure described for **Y-CAU-34**.

Yield and results of the elemental analyses (observed/calculated):

Dy-CAU-34 $([Dy_2(H_2O)_2(C_{26}H_{16}P_4O_{12}H_2)] \cdot 3.5H_2O$, 129 mg, 80.1%): C 30.0/29.7, H 2.91/2.59

Ho-CAU-34: $([Ho_2(H_2O)_2(C_{26}H_{16}P_4O_{12}H_2)] \cdot 2H_2O$, 124 mg, 80.0%): C 30.1/29.8, H 2.84/2.42

Er-CAU-34: $([Er_2(H_2O)_2(C_{26}H_{16}P_4O_{12}H_2)] \cdot 3H_2O$, 120 mg, 74.7%): C 29.5/29.2, H 2.94/2.64

Tm-CAU-34: $([Tm_2(H_2O)_2(C_{26}H_{16}P_4O_{12}H_2)] \cdot 1.5H_2O$, 94.3 mg, 60.0%): C 29.4/29.8, H 2.95/2.41

Yb-CAU-34: $([Yb_2(H_2O)_2(C_{26}H_{16}P_4O_{12}H_2)] \cdot 3H_2O$, 86.8 mg, 53.5%): C 29.3/28.9, H 2.92/2.61

Structure determination

The structure of **Y-CAU-34** was solved from electron diffraction data. The shutterless data collection was performed with continues crystal rotation method (3D-ED/MED) at 645 mm detector distance. The dataset contains 400 frames, which were saved and processed (CrysAlis^{Pro})[25] with a scan width of 0.25° and an exposure time of 0.25 seconds. The completeness of the data was 66.3% at 0.8 Å, which was sufficient to get a crystal structure solution using intrinsic phasing[26] and refine it with kinematic approximation in a partially restrained model.[27] The final ED crystal structure was suitable for a successful Rietveld refinement against PXRD data. Topas Academics[15] was used for the structure refinement. A z-matrix of half a linker molecule as well as distance and angle restraints for Y–O and the C–P–O moieties were used. Details are given in the supporting information.

Deposition Number 2202254 (for **Y-CAU-34**) contains the supplementary crystallographic data for this paper. These data are provided free of charge by the joint Cambridge Crystallographic Data Centre and Fachinformationszentrum Karlsruhe Access Structures service www.ccdc.cam.ac.uk/structures.

Acknowledgements

Financial support by the state of Schleswig-Holstein is acknowledged. The authors thank Mirjam Poschmann, Bastian Achenbach, Jonas Gosch, Niklas Ruser and the spectroscopic section of the department of inorganic chemistry (University of Kiel) for their support with various measurements. We thank Rigaku for the electron diffraction data and Jakub Wojciechowski for the support in processing the data. Open Access funding enabled and organized by Projekt DEAL.

Conflict of Interest

The authors declare no conflict of interest.

Data Availability Statement

The data that support the findings of this study are available from the corresponding author upon reasonable request.

Keywords: Electron diffraction · Metal phosphonate · MOF · Rare earth · Rietveld

[1] a) A. E. Baumann, D. A. Burns, B. Liu, V. S. Thoi, *Commun. Chem.* **2019**, *2*, 1; b) A. Kirchon, L. Feng, H. F. Drake, E. A. Joseph, H.-C. Zhou, *Chem. Soc. Rev.* **2018**, *47*, 8611–8638.
[2] I. Stassen, B. Bueken, H. Reinsch, J. F. M. Oudenhoven, D. Wouters, J. Hajek, V. van Speybroeck, N. Stock, P. M. Vereecken, R. van Schaijk, D. de Vos, R. Ameloot, *Chem. Sci.* **2016**, *7*, 5827–5832.
[3] O. Shekhah, J. Liu, R. A. Fischer, C. Wöll, *Chem. Soc. Rev.* **2011**, *40*, 1081.
[4] J. Yu, C. Mu, B. Yan, X. Qin, C. Shen, H. Xue, H. Pang, *Mater. Horiz.* **2017**, *4*, 557–569.
[5] a) G. K. H. Shimizu, R. Vaidhyanathan, J. M. Taylor, *Chem. Soc. Rev.* **2009**, *38*, 1430–1449; b) K. J. Gagnon, H. P. Perry, A. Clearfield, *Chem. Rev.* **2012**, *112*, 1034–1054.
[6] Y.-P. Zhu, T.-Y. Ma, Y.-L. Liu, T.-Z. Ren, Z.-Y. Yuan, *Inorg. Chem. Front.* **2014**, *1*, 360–383.
[7] a) S. R. Miller, G. M. Pearce, P. A. Wright, F. Bonino, S. Chavan, S. Bordiga, I. Margiolaki, N. Guillou, G. Férey, S. Bourrelly, P. L. Llewellyn, *J. Am. Chem. Soc.* **2008**, *130*, 15967–15981; b) M. Taddei, F. Costantino, F. Marmottini, A. Comotti, P. Sozzani, R. Vivani, *Chem. Commun.* **2014**, *50*, 14831–14834; c) T. Zheng, Z. Yang, D. Gui, Z. Liu, X. Wang, X. Dai, S. Liu, L. Zhang, Y. Gao, L. Chen, D. Sheng, Y. Wang, J. Diwu, J. Wang, R. Zhou, Z. Chai, T. E. Albrecht-Schmitt, S. Wang, *Nat. Commun.* **2017**, *8*, 15369.
[8] S. J. I. Shearan, N. Stock, F. Emmerling, J. Demel, P. A. Wright, K. D. Demadis, M. Vassaki, F. Costantino, R. Vivani, S. Sallard, I. Ruiz Salcedo, A. Cabeza, M. Taddei, *Crystals* **2019**, *9*, 270.
[9] S. Wöhlbrandt, C. Meier, H. Reinsch, E. Svensson Grape, A. K. Inge, N. Stock, *Inorg. Chem.* **2020**, *59*, 13343–13352.
[10] F. Steinke, A. Javed, S. Wöhlbrandt, M. Tiemann, N. Stock, *Dalton Trans.* **2021**, *50*, 13572–13579.
[11] M. Feyand, E. Mugnaioli, F. Vermoortele, B. Bueken, J. M. Dieterich, T. Reimer, U. Kolb, D. de Vos, N. Stock, *Angew. Chem.* **2012**, *124*, 10519–10522; *Angew. Chem. Int. Ed.* **2012**, *51*, 10373–10376.
[12] T. Rhauderwiek, H. Zhao, P. Hirschle, M. Döblinger, B. Bueken, H. Reinsch, D. de Vos, S. Wuttke, U. Kolb, N. Stock, *Chem. Sci.* **2018**, *9*, 5467–5478.
[13] S. Leubner, H. Zhao, N. van Velthoven, M. Henrion, H. Reinsch, D. E. de Vos, U. Kolb, N. Stock, *Angew. Chem. Int. Ed. Engl.* **2019**, *58*, 10995–11000.
[14] B. Wang, T. Rhauderwiek, A. K. Inge, H. Xu, T. Yang, Z. Huang, N. Stock, X. Zou, *Chem. Eur. J.* **2018**, *24*, 17429–17433.
[15] A. A. Coelho, *J. Appl. Crystallogr.* **2018**, *51*, 210–218.
[16] R. A. Coxall, S. G. Harris, D. K. Henderson, S. Parsons, P. A. Tasker, R. E. P. Winpenny, *J. Chem. Soc. Dalton Trans.* **2000**, 2349–2356.
[17] a) P. Z. Moghadam, A. Li, S. B. Wiggin, A. Tao, A. G. P. Maloney, P. A. Wood, S. C. Ward, D. Fairen-Jimenez, *Chem. Mater.* **2017**, *29*, 2618–2625; b) I. J. Bruno, J. C. Cole, P. R. Edgington, M. Kessler, C. F. Macrae, P. McCabe, J. Pearson, R. Taylor, *Acta Crystallogr. Sect. B* **2002**, *58*, 389–397.
[18] J. Guo, X. Xue, H. Yu, Y. Duan, F. Li, Y. Lian, Y. Liu, M. Zhao, *J. Mater. Chem. A* **2022**, *7*, eabg2580.
[19] A. K. Cheetham, C. N. R. Rao, R. K. Feller, *Chem. Commun.* **2006**, 4780–4795.
[20] Y. Q. Jia, *J. Solid State Chem.* **1991**, *95*, 184–187.
[21] R. D. Shannon, *Acta Crystallogr. Sect. A* **1976**, *32*, 751–767.
[22] L. Sarkisov, R. Bueno-Perez, M. Sutharson, D. Fairen-Jimenez, *Chem. Mater.* **2020**, *32*, 9849–9867.
[23] A. F. Ismail, K. C. Khulbe, T. Matsuura, *Gas separation membranes. Polymeric and inorganic*, Springer, Cham **2015**.
[24] N. Stock, T. Bein, *Angew. Chem. Int. Ed.* **2004**, *43*, 749–752; *Angew. Chem.* **2004**, *116*, 767–770.
[25] S. Ito, F. J. White, E. Okunishi, Y. Aoyama, A. Yamano, H. Sato, J. D. Ferrara, M. Jasnowski, M. Meyer, *CrystEngComm* **2021**, *23*, 8622–8630.
[26] G. M. Sheldrick, *Acta Crystallogr. Sect. A* **2015**, *71*, 3–8.
[27] O. V. Dolomanov, L. J. Bourhis, R. J. Gildea, J. A. K. Howard, H. Puschmann, *J. Appl. Crystallogr.* **2009**, *42*, 339–341.

Manuscript received: August 29, 2022
Revised manuscript received: September 30, 2022